Asian Review of Mechanical Engineering
ISSN: 2249-6289 (P) Vol.2 No.2, 2013, pp.19-26

DOI: https://doi.org/10.51983/arme-2013.2.2.2350

Comparative Study on Corrosion Behavior of SA213T22 and SA213T91 Steels in Molten Salt Environment of Na_2SO_4-60% V_2O_5 at 900°C

Rutash Mittal[1], Lucky Goyal[2] and Buta Singh Sidhu[3]

[1]*Department of Mechanical Engineering, Malout Institute of Management & Information Technology, Malout, Dist. Sri Muktsar Sahib - 152 107, Punjab, India*

[2]*Research Scholar, Applied Sciences Department (Physics), Punjab Technical University, Kapurthala,Punjab, India*

[3]*Dean Academics, Punjab Technical University, Jalandhar-Kapurthala Highway, Kapurthala, Punjab, India*

Email: butasidhu@yahoo.com, rutashmittal@gmail.com

Abstract **– The hot corrosion behavior of boiler tube steels SA213T91 (T91) and SA213T22 (T22) after exposure to molten salt of Na_2SO_4 - 60% V_2O_5 were investigated at a temperature of 900°C in a cyclic manner. Thermo-gravimetric technique was used to establish oxidation kinetics for T91 and T22 steels in salt at 900°C under cyclic conditions for 50 cycles. X-ray diffraction (XRD) and scanning electron microscopy/ Energy dispersive spectrometry (SEM/EDS) techniques were used to characterize the oxide scales. The hot corrosion behavior of T91 steel was found to be better than T22 steel exposed to oxidation under salt condition.**

Keywords**: Boiler Steel T91, T22, Hot Corrosion, Na_2SO_4 - 60% V_2O_5, SEM/EDS, XRD**

I. Introduction

Many components used in thermal power plants, various power generating industries and mills have to operate under severe conditions such as high load, speed, temperature and hostile chemical environment. According to the findings of Uustilo and co-workers [1], the power plants are one of the major industries suffering from severe corrosion problems resulting in the substantial losses. The performance of materials used in high-temperature environments is related to their ability to form protective oxide scales on their surfaces. Metals and alloys experience accelerated oxidation when their surfaces are covered with a thin film of a fused salt in an oxidizing environment at elevated temperature. This mode of attack is commonly known as hot-corrosion, which takes place at an accelerated rate [2]. A common manifestation of hot-corrosion at elevated temperatures is the development of a porous non-protective oxide scale and sulphide precipitates in the substrate [3]. In coal fired boilers and power generating plants, corrosion at elevated temperature is recognized as the main cause of down time. So, the behavior of materials at elevated temperature is gaining technological importance

Ferritic steels, containing chromium and molybdenum are well known for their excellent mechanical properties combining high temperature strength and creep resistance with high thermal fatigue life, as well as with good thermal conductivity, weldability, and resistance to corrosion. Because of these characteristics this type of steels have attracted special interest for application in industrial processes related to carbo-chemistry, oil refining, carbon gasification and energy generation in thermal power plants, where components like, heat exchangers, boilers and pipes operate at high temperatures and pressures for long periods of time[4,5].

Amongst these the T22 and T91 ferritic steels have widespread use in the boilers of power plants of northern India. As per the actual study of boiler of unit-4 of G.N.D.T.P. bathinda, Punjab, India T22 metal is used in the primary section and T91 is used in the secondary section of the boiler. At high temperature exposure the interaction between a metal or an alloy and the surrounding gases and combustion products leads to corrosion, thus leading to failure for materials and structures [6, 7]. It is commonly reported that as a result of the oxidation process under isothermal conditions a protective Cr-containing oxide and Fe-containing oxide is developed over the surface of the steel causing a decrease of the oxidation rate with time. Oxide scale is constituted by a layered structure with compositional and microstructural variations from

the substrate to the outer interface [8]. On the other hand, depending on the oxidation temperature and the chemical composition of the steel, both, the mechanisms of formation and the microstructural characteristics of the oxide scale, along with the degree of protection it provides, are different [9].

This paper is an effort for the knowledge of the corrosion behavior of the T91 and T22 ferritic steels in salt atmosphere of Na_2SO_4-60%V_2O_5 at temperature of 900°C in cyclic manner. This experimental study is the part of the work carried by the authors in the study of dissimilar metal weldments exposed to high temperatures in boilers of power plants.

II. Experimental Procedure

A. Substrate Material

Two types of substrate materials namely SA213T91 (T91) and SA213T22 (T22) were used. These materials are used as boiler tube materials in some of power plants in northern India. When the service conditions are stringent from the point of temperature and pressure, these steels find wide applications in power plants and other higher temperature operative industries. The chemical composition of these steels is reported in Table I.

Table I* Chemical Composition (Wt. %) of The Metals

Metal	C	Cr	Mn	Mo	Si	V	Fe
SA213 T91	0.096	8.76	0.47	1.03	0.37	0.26	Bal.
SA213 T22	0.127	2.18	0.43	0.94	0.35	0.02	Bal.

*The actual chemical composition of the base metals was analyzed with the help of Optical Emission Spectrometer of (TJA 181/81) at Metallurgical & Materials Engineering. Dept.,I.I.T. Roorkee, Uttra-Khand, India.

B. Sample Preparation

The experiment was performed on samples which were made to specified dimensions of approximately 40 x 12 x 3.5 mm^3 from tubular sections. The specimens were polished on SiC emery paper down to 2000 from 80 grades and finally cloth polishing with alumina paste on rotating disc. Polishing was carried out on all six faces. The specimens were degreased (by ultrasonic cleaning in ethanol) and dried, then they were accurately weighed and measured to determine the total surface area exposed to the oxidative environment.

C. Optical Microscopy

The microstructure of the T91 and T22 steel samples were revealed after following a standard metallographic procedure of polishing and etching. The microstructure of T22 was revealed with 5% nital solution (5% HNO_3 and 100ml ethyl alcohol) and that of T91 with marble's reagent ({$CuSo_4$(4gm)+ HCl(20ml)+distilled water(20ml)} As depicted in Figure 1(a) the microstructure of T91 consists of tempered lath martensite. The prior austenite grain boundaries as well as lath boundaries are decorated with precipitates, the white spots represent the ferrite phase and rest is other phase [10]. T22 sample revealed the microstructure shown in Fig. 1(b), which was found to consist of white ferrite and black pearlite.

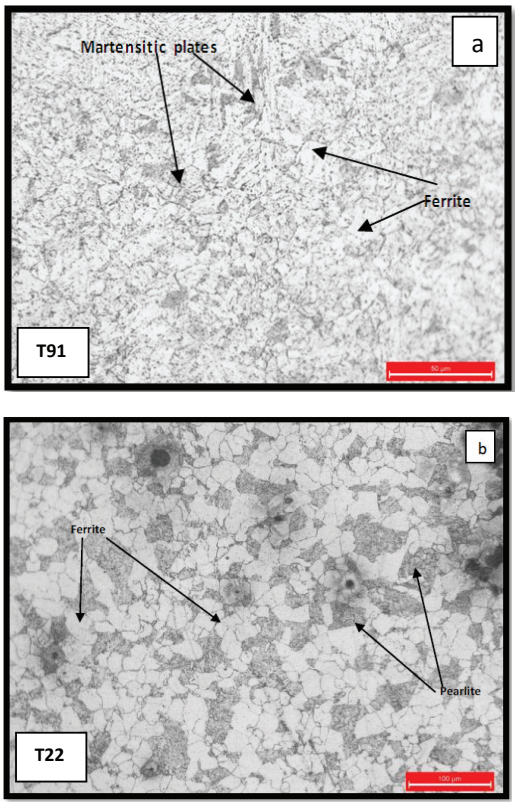

Fig. 1 Microstructure of substrates (a) T91 and (b) T22

D. Molten Salt Corrosion Test

Salt (Na_2SO_4- 60%V_2O_5) for 50 cycles under cyclic conditions. Each cycle consisted of 1h heating at 900°C in a silicon carbide tube furnace followed by 20 min cooling at room temperature. The furnace was calibrated to an accuracy of ±5°C using a platinum/platinum–13% rhodium thermocouple. The purpose of imposed cyclic loading was

to create severe conditions for testing as these conditions constitute more realistic approach towards solving the problem of metal corrosion in actual applications [11, 12]. The cyclic study was performed for 50 cycles as this duration is considered to be adequate to achieve the steady state of oxidation for most of the materials [13, 14]. The studies were performed for both the specimens for comparison. Before testing the physical dimensions of the specimen were recorded carefully with a digital vernier caliper (Mitutoyo, Japan make, resolution 0.01 mm) to evaluate their surface areas. Thereafter, the sample was heated in an oven up to 250 °C and the salt mixture of Na_2SO_4–60%V_2O_5 dissolved in distilled water was coated on all over the surface of warm sample with the help of a camel hair brush. The heating of the specimen was found essential for proper adhesion of the salt layer. The amount of the salt coating varies in the range 3.0–5.0 mg/cm^2. The salt coated sample was then dried at 100°C for 3–4h in the oven to remove the moisture. Subsequently, the dried salt coated specimen kept in the alumina boat was weighed before exposing to hot corrosion tests in the tube furnace kept at 900°C. The alumina boats used for the study were preheated at a constant temperature of 1000°C for 8h so that their weight would remain constant during the course of high temperature cyclic study. During hot corrosion runs, the weight of boat and specimen was measured together at the end of each cycle with the help of an electronic balance of model Prism xt (FIE, India) having sensitivity of 0.1 mg. During each cycle, the data taken for the sample was used to calculate the corrosion rate. The spalled scale if any was also included in weight change measurements. The kinetics of corrosion was determined from the weight change measurements. Visual observations were also made after the end of each cycle with regard to color, luster, adherence/spallation tendency and any other physical aspect of the oxide scales/coatings. After the hot corrosion studies, the corroded samples were analyzed by using XRD and SEM/EDS techniques. The corroded samples were cut using slow speed cutter (GEM model of Precision Industries, New Delhi, India) across the cross-section and cold mounted in transparent powder for the cross-sectional analysis using SEM/EDS and elemental X-ray mapping.

Scanning electron microscope (SEM) of JEOL Japan make having model JSM-6610LV equipped with EDS of oxford instruments facility having model number 51-ADD0013 installed at IIT Ropar is used to study the micrographs of the samples. X ray diffraction facility of IIT Ropar using Instrument of PAN Alytical, Model X'Pert PROMPD made in Neitherland is also used to have XRD of the specimens.

III. Results

A. Visual Examination

The surface macrographs of the substrate steels T91 and T22 after some stipulated cycles are shown in Fig.2 and Fig. 3 respectively. The oxide scale formed on T91 substrate after 10 cycles is very fine and blackish grey in color, the physical condition of substrate remains somewhat similar till 30 cycles. Violet and grey coloured scale is observed on surface of substrate after 40 cycles. Ultimately after 50 cycles the scale looks black in color with grey spots. The sputtering sound was observed whenever the boat is taken out from the furnace and put in air. The substrate T22 develops brown and grey scale after 10 and 20 cycles. The T22 substrate develops cracks on the edges and corners of the sample by completion of 10 cycles. The sputtering and peeling off of the scale layers start after 20 cycles which adds to increase in weight. After 40 and 50 cycles of studies more and more layers of oxides exfoliated and removed from T22 substrate and falls in the boat. The physical condition of the T22 sample after complete studies looks badly deteriorated having many laminated layers of oxide peeled off from the surface of the metal surface. The mechanism responsible for the removal of layers of oxide from the T22 substrate is removal of oxide flakes in continues manner. The oxidative flakes are thick, porous and non-protective with plenty of Fe in the oxide scale fallen in the boat (Fig. 3a, 6a). The observed corrosion rate of T91 seems to be less in comparison to T22 substrate.

B. Thermo-Gravimetric Data Analysis

Thermo-gravimetric data for boiler steels subjected to cyclic oxidation is presented in Fig.4 (a) in the form of a graph between weight gain per unit area (mg/cm^2) versus time expressed in number of cycles. The mass change data serve as a good index to compare the corrosion rates under similar conditions of exposure. It can be inferred from the plot that the substrate steel T91 steel showed mass gains was parabolic until the end of the exposure. On the other hand, in case of substrate steel T22 the mass gain showed deviation from parabolic behavior. It is obvious from the weight gain graph that T22 steel has shown much higher corrosion rates as compared to T91 steel. Comparative analysis indicate that the T22 steel has the tendency to have higher mass gain continuously without showing any indication of steady state corrosion rate. The graph between (weight gain/area)^2 versus number of cycles for T91 and T22 substrates is shown in Fig. 4(b), which depicts that T91 substrate follows the parabolic law whereas T22 substrate shows some deviation from the

parabolic rate law. The cumulative weight gain of both the substrates presented in Fig. 4(c) depicts the higher weight gain of 73.89 mg/cm^2 for T22 substrate than weight gain of 15.88mg/cm^{2}for T91 substrate.

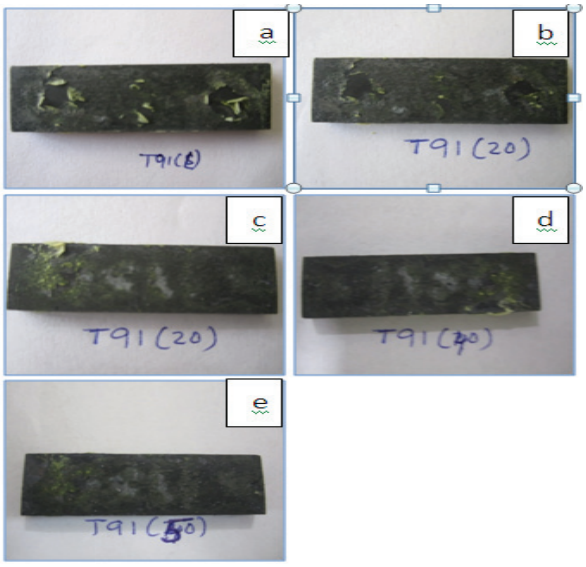

Fig. 2 Surface macrographs for the boiler steel T91 subjected to hot corrosion in molten salt of (Na_2SO_4- 60%V_2O_5) at 900^{o}C for (a) 10 cycles (b) 20 cycles (c) 30 cycles (d) 40 cycles (e) 50 cycles

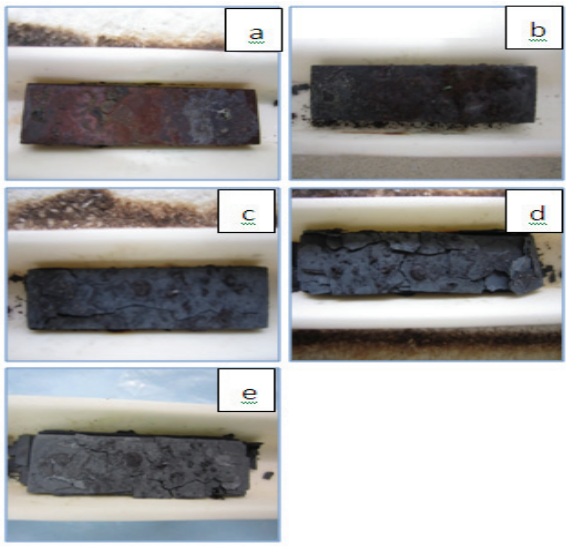

Fig. 3 Surface macrographs for the boiler steel T22 subjected to hot corrosion in molten salt of (Na_2SO_4- 60%V_2O_5) at 900^{o}C for (a) 10 cycles (b) 20 cycles (c) 30 cycles (d) 40cycles (e) 50 cycles.

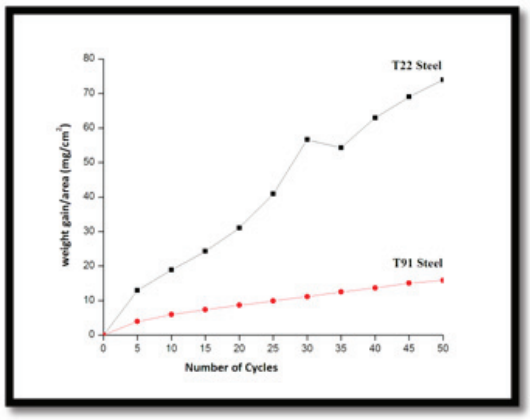

Fig.4 (a) Weight gain per unit area vs. number of cycles plot for boiler steels T91 and T22 subjected to cyclic oxidation in molten salt at 900oC for 50 cycles

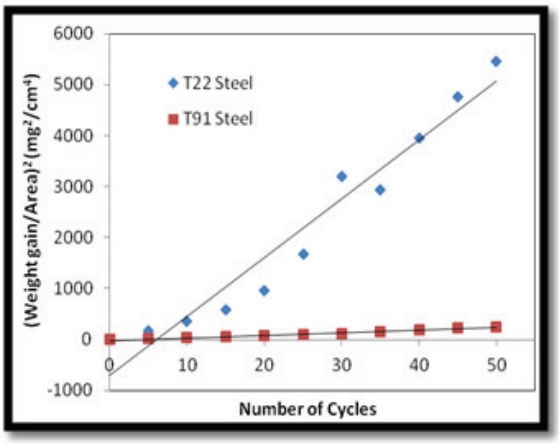

Fig.4 (b) (weight gain/area)^2 vs. Number of cycles plot for T91 and T22 boiler steels subjected to cyclic oxidation in molten salt at 900^{o}C for 50 cycles

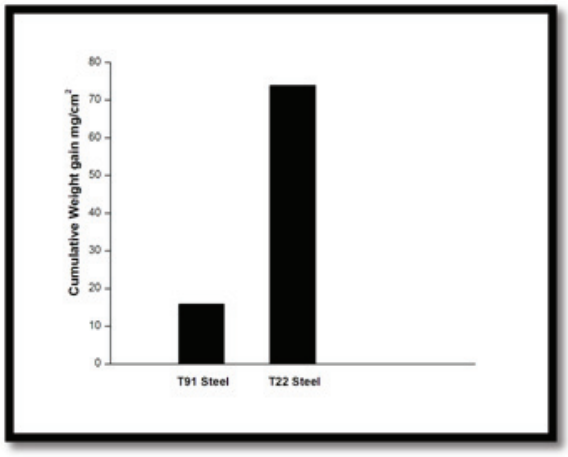

Fig.4 (c) Bar chart showing cumulative weight gain for T91 and T22 boiler steel subjected to cyclic oxidation in molten salt at 900^{o}C for 50 cycles

C. XRD Analysis of the Exposed Samples

The XRD patterns for T22 and T91 substrate steels subjected to cyclic oxidation in molten salt of Na_2SO_4-60%V_2O_5 at 900°C for 50 cycles are depicted in Fig.5. As indicated by the XRD patterns Fe_2O_3 is observed to be the main phase along with minor presence of Fe_3O_4 in the oxide scale of T22 boiler steel. In case of T91 boiler steel, the formation of Fe_2O_3 and Cr_2O_3 as major phase has been indicated by XRD peaks. Minor peaks pertaining to presence of $(Cr, Fe)_2O_3$, $NiCr_2O_4$, $NiFe_2O_4$ and FeV_2O_4,MoO_2, FeS, CrS are also observed.

D. SEM/EDS Analysis of The Exposed Specimens

1. *Surface Analysis of the Scale*

SEM micrographs along with EDS analysis for substrate steels T22 and T91 subjected to cyclic oxidation in molten salt Na_2SO_4-60%V_2O_5 at 900°C for 50 cycles are shown in Figs. (6a, 6b) respectively. The oxide scale on the surface of T22 steel has a melted area and layered format of scale is observed which is composed mainly of Fe and O, thereby indicating the formation of Fe_2O_3 rich oxide scale. The oxide scale observed on the surface of T91 steel seems to be uniform and well adhered. The EDS analysis depicts the major presence of Fe, Cr, O and minor presence of other reacting species justified by the XRD of surface of T91 steel. The surface morphology of T22 steel exposed sample is fibrous and discontinuous in nature. As compared to T22 steel large presence of Cr on T91 steel is analogues to the formation of protective Cr_2O_3 phase on the substrate which is mainly responsible for the corrosion protection of the material.

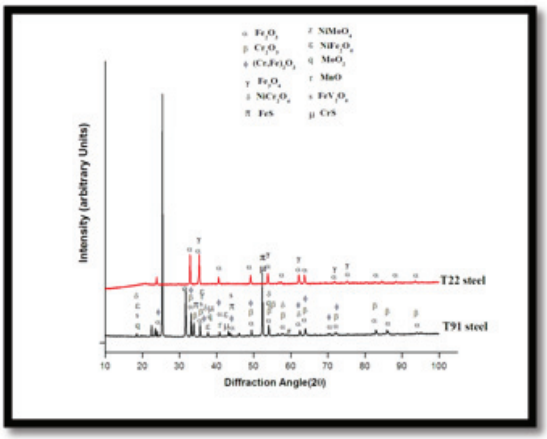

Fig.5 XRD plot for boiler steels T91and T22 subjected to cyclic oxidation in molten salt at 900°C for 50 cycles.

2. *Cross- Sectional Analysis of the Scale*

The SEI image showing the cross sectional oxide scale morphology and corresponding EDS analysis at some selected points of the T91 and T22 substrates subjected to molten salt of Na_2SO_4-60%V_2O_5 at 900°C for 50 cycles have been compiled in Fig. 7(a, b). The scale in this paper has been referred as the material present above the substrate steel, which may include oxidized/ partially oxidized layers plus any other layer found on the surface, as could be seen from the cross-sectional micrographs. As per cross-sectional SEM micrograph of hot corroded T91 steel and its compositional elemental point analysis shown in Fig.7 (a), the penetration of O and other elements can be analyzed. The penetration of O and S in the substrate is limited. While moving from the substrate to oxide layer elemental percentage of O is seen along with the presence of Fe and Cr which justifies the formation of ferrous oxide Fe_2O_3 and Cr_2O_3. This postulates the outward diffusion of Fe and Cr from the substrate to oxide layer. While moving from point 5 to point 6 minor increase in composition of Fe and Cr is observed. In the cross-sectional SEM micrograph and compositional elemental point analysis of hot corroded T22 steel depicted in Fig. 7(b), it is observed that penetration of corroding species like O is very high even in the substrate. Due to the presence of higher percentage of O and small amount of other species a subscale region is formed before the actual external oxide layer. Although Cr is present to a very small amount in T22 steel but nearly negligible amount of Cr is observed in the oxide scale of T22 steel. Mainly Fe and O are observed which justify the presence of Fe_2O_3 and Fe_3O_4 in the outer scale. The presence of these phases is reported to be non protective by Das *et. al.* [15].

3. *X-ray Mapping of Exposed Specimens*

Compositional Image (SEI) and X-ray mapping of the cross-section of hot corroded T91 and T22 substrates subjected to Na_2SO_4-60%V_2O_5 at 900°C for 50 cycles have been presented in Figs. 8, 9 respectively. The analysis of T91 steel in Fig. 8 indicates that the base metal is mainly composed of Fe and some percentage of Cr. The oxide scale of the T91 steel has the presence of O, Fe and Cr confirming the presence of Fe_2O_3 and Cr_2O_3 as major phase, where as the minor presence of Ni, S, V, Na and Mo is also observed. Minor presences of these elements is said to responsible for the minor phases of $(Cr, Fe)_2O_3$, $NiCr_2O_4$, $NiFe_2O_4$ and FeV_2O_4,MoO_2, FeS, CrS. The oxide scale morphology in

the x-ray mapping depicts the intact and adhered nature of the scale with some cracks observed parallel to the substrate surface. The analysis of T22 steel in Fig. 9 indicates that the substrate is mainly composed of Fe. The oxide scale of the T22 steel has main presence of Fe and O indicating the presence of Fe_2O_3 phase. The minor presence of Cr, S, V, Na and Mo is also observed in the outer scale of the substrate. The morphology of the oxide layer of T22 steel in x-ray mapping shows the layered and loosely bound nature of the scale. The penetration of O and other species till the substrate is observed which causes the oxidation of the substrate and formation of a subscale oxide layer in the substrate. This type of behavior is not good for the corrosion resistance of the metal.

IV. Discussion

The corrosion of the both substrates is observed under the influence of environment of Na_2SO_4-60%V_2O_5 at 900°C for 50 cycles. The T22 substrate showed higher rate of corrosion in comparison to its counterpart T91 (Fig. 4a, 4b, 4c). Kotla et. al. [16] described that Na_2SO_4 and V_2O_5 will react at 900^0C to form $NaVO_3$ which acts as a catalyst and works as an oxygen carrier to the substrate through pores present on the surface, which causes oxidation of elements of the substrate. Internal oxidation of T22 substrate has promoted the cracking and spalling of scale due to difference in thermal coefficients of oxides in the scale from the substrate [17]. Through pores on the surface and cracks in oxide layer, corrosive gases can penetrate to the substrate and allow significant grain boundary corrosion attack [11, 18]. Fe_2O_3 was observed to be the main phase (Fig. 5) in the oxide scale of T22 substrate. This was further supported by SEM/EDS analysis (Fig. 6a), which presents higher amount of Fe and O on the surface of scale of T22 substrate. The presence of Fe_2O_3 scale is being reported to be non-protective in nature [16]. The results of XRD and SEM/EDS analysis for hot corroded T22 substrate are also corroborated by the cross-sectional point analysis (Fig. 7b) and x-ray mapping (Fig. 9), which reveals the prominent presence of O and Fe in the outer scale.

The XRD analysis of T91 substrate (Fig. 5) after corrosion studies revealed the presence of Fe_2O_3 and Cr_2O_3 as major phases along with some phases of $NiCr_2O_4$ and $(Cr, Fe)_2O_3$. The latter oxides are known for providing superior corrosion resistance as reported by Ul-hamid, T.S.Sidhu and T. sundarajan in their research [19, 20, and 22]. Moreover the surface SEM/EDS analysis (Fig. 6b) of oxide of T91 substrate along with cross-sectional point analysis (Fig. 7a) and elemental x-ray mapping (Fig. 8) supported the formation of these oxides reported in XRD analysis of T91 substrate. Which showed that scale is primarily composed of Fe, Cr and O elements. The presence of spinel phase in the oxide scale will further enhance the corrosion resistance, as spinel phases have much lower diffusion coefficients of the cations and anions than those in the oxide phases of Fe [21, 23]. Hence the corrosion behavior of T91 substrate is observed to be better than T22.

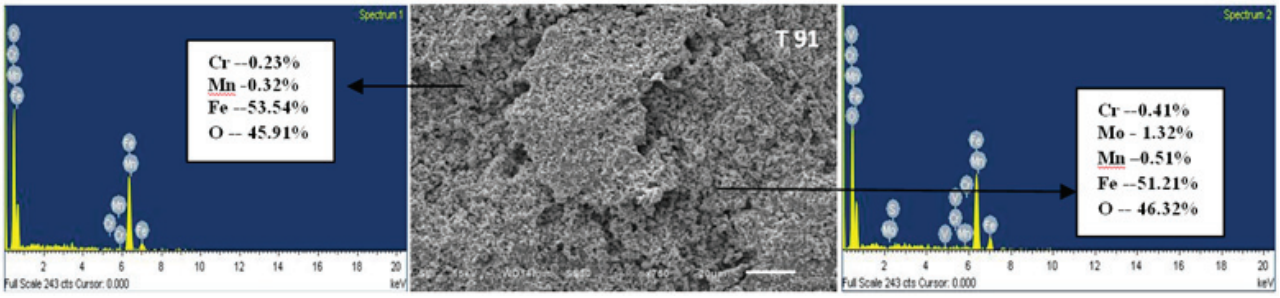

Fig.6 (a) SEM/EDS analysis of T22 subjected to molten salt of Na_2SO_4-60%V_2O_5 at 900^0C

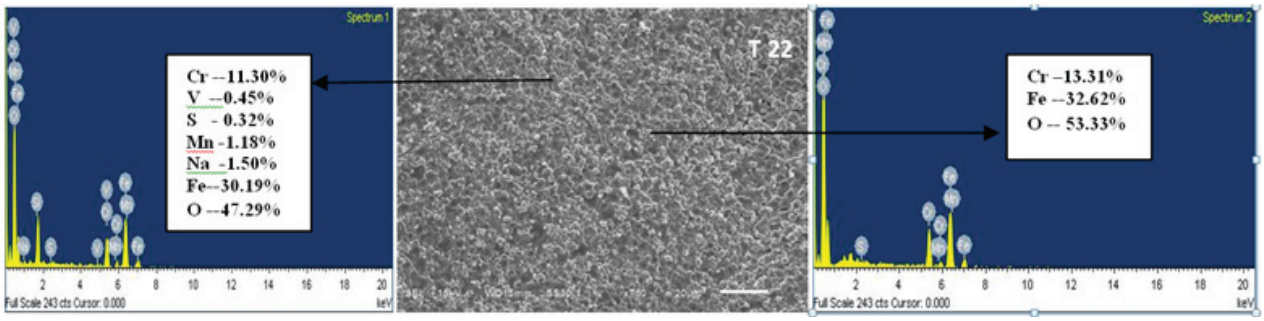

Fig. 6(b) SEM/EDS analysis of T91 subjected to molten salt of Na_2SO_4-60%V_2O_5 at 900^0C

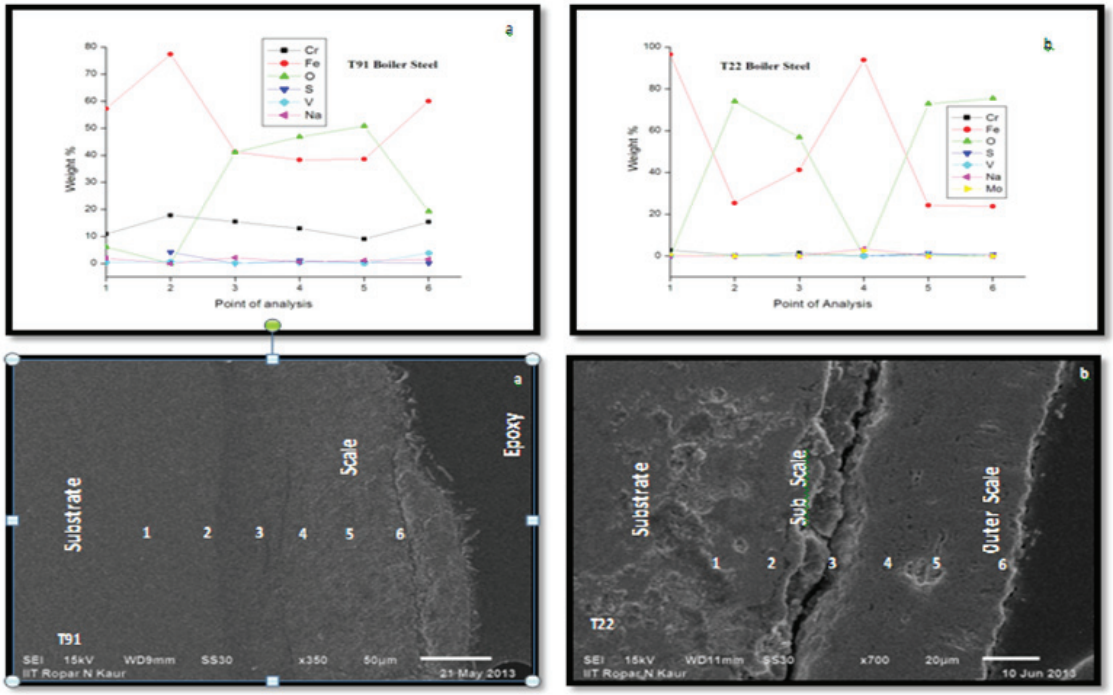

Fig. 7(a, b) SEI micrograph and variation in compositional elements across the cross section of the hot corroded substrates (a) T91 and (b) T22

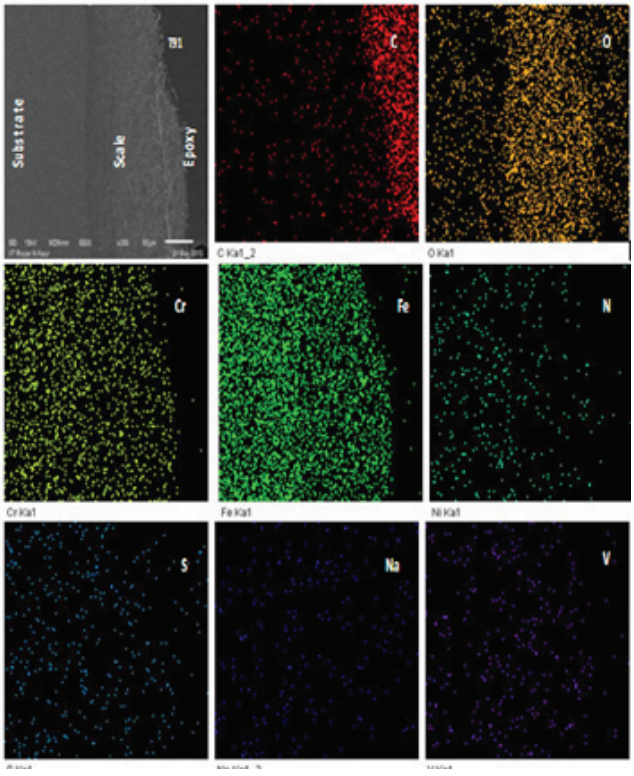

Fig.8 SEI and elemental X-ray mapping of the cross-section of T91 sample exposed to cyclic hot corrosion in Na2SO4-60%V_2O_5 at 900°C for 50 cycles.

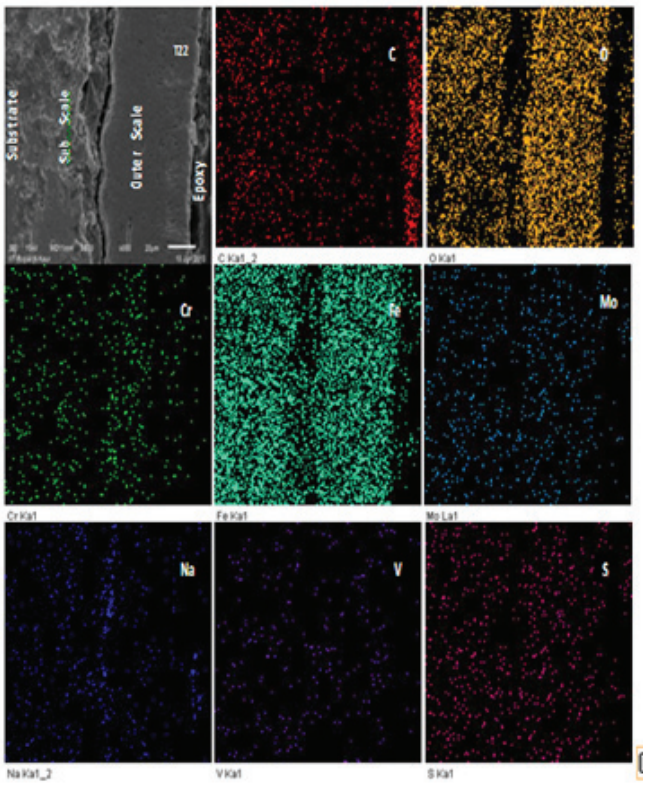

Fig.9 SEI and elemental X-ray mapping of the cross-section of T22 sample exposed to cyclic hot corrosion in Na2SO4-60% V_2O_5 at 900°C for 50 cycles.

V. CONCLUSIONS

The cyclic oxidation of T91 substrate in molten salt follows parabolic rate of weight gain whereas T22 substrate show some deviation from the parabolic nature. The better corrosion resistance of T91 substrate steel is due to the presence of Cr_2O_3 and spinels of $NiCr_2O_4$ and (Cr, $Fe)_2O_3$ phases, which are protective to process of oxidation. It approves the technical fact of using T91 metal in higher and stringent conditions and using T22 metal in somewhat lower temperature ranges of boiler of power plants.

References

[1] M.A. Uustilo, P. M. J. Vuoristo and T.A. Mantyla, Material Science Engineering A- Struct., 346 (2003),No. 1-2, pp. 168-177.

[2] N. Eliaz, G. Shemesh and R. M. Latanision, Engineering Failure Analysis 9, 31 (2002).

[3] R. A. Rapp, Y. S. Zhang, JOM 46, 47 (1994).

[4] J.C. Van Wortel, C.F. Etienne, F. Arav, Application of modified 9 chromium steels in power generation components, in: VDEh ECSC Information Day, The Manufacture and Properties of Steel 91 for the Power Plant and Process Industries, Dusseldorf, 5th November, 1992, paper 4.2.

[5] T. Fujita, Current progress in advanced high Cr steel for high temperature applications ISIJ Int. 32 (2) (1992), p.175.

[6] G.E. Birchenall, A brief history of the study of oxidation of metals and alloys, in: High Temperature Corrosion, Proceedings, NACE, San Diego, CA, 1981, p.3.

[7] D.A. Jones, Principles and Prevention of Corrosion, second ed., Prentice Hall, USA,1996.

[8] A.S. Khanna, P. Rodriguez, J.B. Gananamoorthy, Oxidation kinetics, breakaway oxidation, and inversion phenomenon in 9Cr–1Mo steels, Oxid. Met. 26 (3, 4) (1986) p.171.

[9] Dionisio Laverde, Tomas Gomez-Acebo ,Francisco Castro, Continuous and cyclic oxidation of T-91 ferritic steel under steam, *Corrosion Science* 46 ,2 July 2003, pp.613–631.

[10] Rutash Mittal and Buta singh sidhu, Evaluation of Metallurgical and Mechanical Properties of Dissimilar Metal Weldments of Ferritic SA213T91 and Austenitic AISI347H steels, Materials & Design (Communicated)

[11] S.E. Sadique, A.H. Mollah, M.S. Islam, M.M. Ali, M.H.H. Megat, S. Basri, Oxid. Met. 54 (2000) 385.

[12] B.S. Sidhu, S. Prakash, Oxid. Met. 63 (2005) 241.

[13] N. Bala, H. Singh, S. Prakash, Appl. Surf. Sci. 255 (2009) 6862.

[14] T.S. Sidhu, S. Prakash, R.D. Agrawal, Surf. Coat. Technol. 201 (2006) 792.

[15] D. Das, R. Balasubramaniam and M. N. Mungole, *Journal of Materials Science*, Vol. 37, 1135 (2002).

[16] G. A. Kolta, I. F. Hewaidy and N. S. Felix, Thermochimica Acta 4, 151 (1972).

[17] P. Niranatlumpong, C.B. Ponton, H.E. Evans, Oxid. Met, 53 (3–4) (2000), pp. 241-258.

[18] D. Wang, Surf. Coat. Technol. 36 (1988) p.49.

[19] A-Ul-Hamid, Mater. Chem. Phys. 80 (2003) 135.

[20] T.S. Sidhu, S. Prakash, R.D. Agrawal, Scr. Mater. 55 (2006) 179.

[21] U. K. Chatterjee, S. K. Bose and S. K. Roy, Environmental Degradation of Metals, (Marcel Dekker, New York, 2001).

[22] T. Sundararajan, S. Kuroda, T. Itagaki and F. Abe, ISIJ International 43, 104 (2003).

[23] G. Kaushal, H. Singh and S. Prakash, Oxid Met (2011) 76:169-191.